

Isotropic superconducting gaps with enhanced pairing on electron Fermi surfaces in FeTe_{0.55}Se_{0.45}

H. Miao,¹ P. Richard,¹ Y. Tanaka,² K. Nakayama,² T. Qian,¹ K. Umezawa,² T. Sato,^{2,3} Y.-M. Xu,⁴ Y. B. Shi,¹ N. Xu,¹
 X.-P. Wang,¹ P. Zhang,¹ H.-B. Yang,⁵ Z.-J. Xu,⁵ J. S. Wen,⁵ G.-D. Gu,⁵ X. Dai,¹ J.-P. Hu,^{1,6}
 T. Takahashi,^{2,7} and H. Ding^{1,*}

¹Beijing National Laboratory for Condensed Matter Physics, and Institute of Physics, Chinese Academy of Sciences, Beijing 100190, China

²Department of Physics, Tohoku University, Sendai 980-8578, Japan

³TRiP, Japan Science and Technology Agency (JST), Kawaguchi 332-0012, Japan

⁴Materials Sciences Division, Lawrence Berkeley National Laboratory, Berkeley, California 94720, USA

⁵Condensed Matter Physics and Materials Science Department, Brookhaven National Laboratory, Upton, New York 11973, USA

⁶Department of Physics, Purdue University, West Lafayette, Indiana 47907, USA

⁷WPI Research Center, Advanced Institute for Materials Research, Tohoku University, Sendai 980-8577, Japan

(Received 22 December 2011; published 6 March 2012)

We used angle-resolved photoemission spectroscopy to reveal directly the momentum distribution of the superconducting gap in FeTe_{1-x}Se_x, which has the simplest structure of all Fe-based superconductors. We found isotropic superconducting gaps on all Fermi surfaces whose sizes can be fitted by a single gap function derived from a strong coupling approach, promoting local antiferromagnetic exchange interactions as a serious candidate for the pairing origin.

DOI: [10.1103/PhysRevB.85.094506](https://doi.org/10.1103/PhysRevB.85.094506)

PACS number(s): 74.70.Xa, 74.20.Mn, 74.25.Jb

I. INTRODUCTION

Electronic spin fluctuations are widely believed to be critical to superconductivity in the new Fe-based high-temperature superconductors due to the proximity between the superconducting (SC) and the magnetic ordered phases. The driving mechanisms of both magnetic ordering and superconductivity are currently under intensive debate, mainly between two approaches: a weak coupling approach where both magnetic and SC orders are driven by the enhanced spin susceptibility near the Fermi surface (FS), and a strong coupling approach where the two orders are caused by local magnetic exchange interactions between neighboring electrons. The weak coupling approach has found support from the observation of quasi-nesting between hole FS pockets at the Brillouin zone (BZ) center and electron FS pockets located at the antiferromagnetic wave vector in most ferropnictides.¹⁻⁵ However, this approach has encountered difficulty in explaining the bicollinear magnetic ordering pattern in the ferrochalcogenide FeTe⁶ and it was seriously challenged by the recent observation of isotropic SC gaps in a new ferrochalcogenide superconductor, A_xFe₂Se₂ (A = K, Rb, Cs, Tl), without FS nesting on the particle-hole channel.⁷⁻⁹ On the other hand, the strong coupling approach (e.g., J_1 - J_2 - J_3 model) fares better in explaining the two examples above.^{10,11}

Precise information on the pairing strength along different FS pockets of ferrochalcogenide superconductor FeTe_{1-x}Se_x can be used to distinguish these two approaches due to its close relationship to its magnetic parent FeTe and SC cousin K_xFe₂Se₂. Here we report high-resolution ARPES results on high-quality FeTe_{0.55}Se_{0.45} SC samples. We observe isotropic SC gaps on both electronlike and holelike FS pockets. More importantly, the pairing strength is found to be stronger on the electronlike FSs, which can be naturally explained by the enhanced antiferromagnetic exchange between the third nearest neighbors (J_3) in this material. All the different SC gaps can be fitted by a single gap function that is fully consistent with the strong coupling J_1 - J_2 - J_3 approach.

II. EXPERIMENT

High-quality single crystals were grown by a unidirectional solidification method with a nominal composition of FeTe_{0.55}Se_{0.45} ($T_c = 14.5$ K and $\Delta T_c = 1$ K, as determined by magnetic susceptibility). ARPES measurements were performed at Tohoku University using a VG-Scienta SES 2002 multichannel analyzer and the He I α resonance line of a helium discharge lamp ($h\nu = 21.218$ eV). Additional data were recorded at the Synchrotron Radiation Center (Stoughton, WI) with a VG-Scienta SES 200 using 52 eV light with tunable polarization, as well as at the National Light Source of Brookhaven National Laboratory using a VG-Scienta SES 2002 multichannel analyzer with 16 eV photons. The energy resolution and momentum resolution are set at 2 meV and 0.2° for the measurements of the SC gap. All preparation procedures for the gap measurements were done in a glove box filled with He gas to avoid contact with air. Clean surfaces were obtained by cleaving samples *in situ* in a working vacuum better than 1×10^{-10} Torr.

III. RESULTS AND DISCUSSION

We start with the ARPES experiment of two cuts which include the Γ point and the M point ($\pi, 0$), here defined in the 1 Fe per unit cell notation, respectively. Figures 1(a) [1(c)] and 1(b) [1(d)] show the intensity plots near Γ (M) along the Γ -M direction in the normal state (25 K) and SC state (6 K), respectively. The corresponding energy distribution curves (EDCs) are given below each panel. Around the Γ point, the normal state data show clearly two intense holelike bands. While the inner one (α) sinks ~ 14 meV below E_F , the outer one (α') crosses E_F very close to Γ . A third weaker holelike band with a larger Fermi wave vector (k_F) and a larger effective mass, named β band, is also visible. Around the M point, one electron pocket (γ) with a smaller effective mass is also resolved. Upon cooling temperature below $T_c = 14.5$ K, SC coherent peaks develop on the α' , β ,

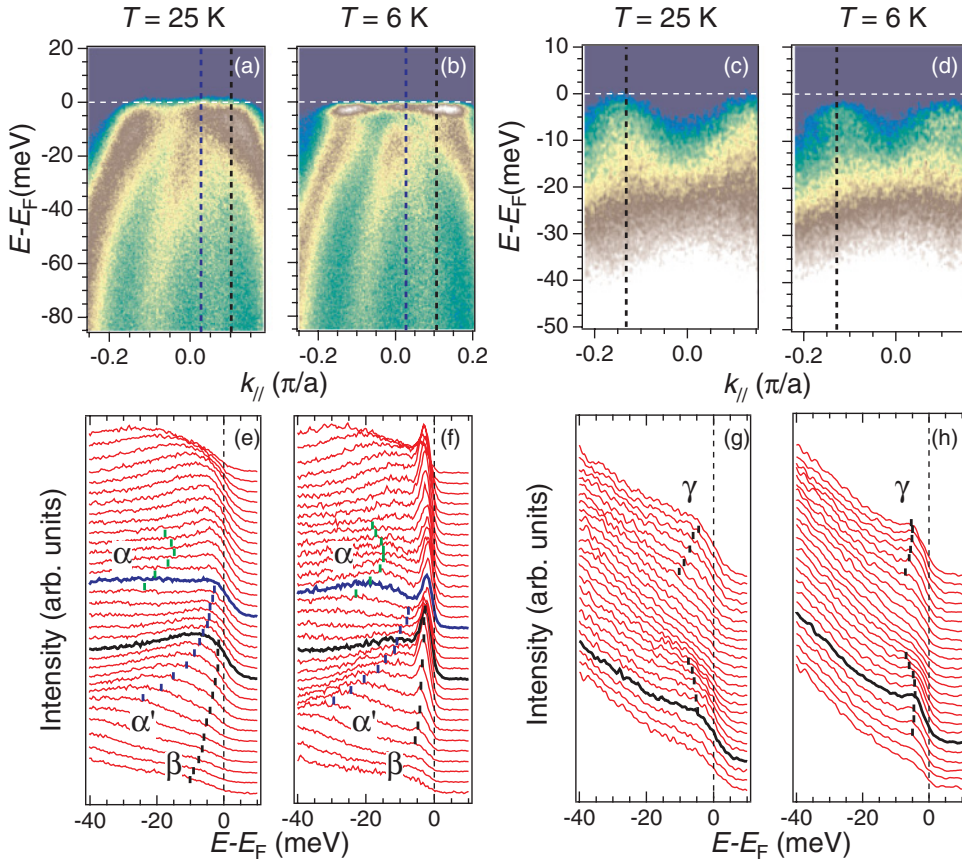


FIG. 1. (Color online) (a)–(d) ARPES intensity plots along Γ -M. (a) Near Γ , in the normal state ($T = 25$ K). Blue and black dotted lines indicate the k_F positions of the α' and β bands, respectively. (b) Same as (a) but in the SC state ($T = 6$ K). (c) Near M, normal state ($T = 25$ K). (d) Near M, SC state ($T = 6$ K). The corresponding EDCs are given below each panel in (e)–(h). Thick bars are guides for the eye.

and γ bands, as well evidenced by the low temperature EDCs shown in Figs. 1(f) and 1(h). The temperature evolution of the coherent peaks is drastic and confirms their SC origin. The temperature dependence of the EDC recorded at a particular k_F of the β band is displayed in Fig. 2(a), which shows dramatic line shape change across T_c . The impressive sharpness of these SC coherent peaks (full width at half maximum < 5 meV) compared to a previous ARPES study¹² on FeTe_{0.7}Se_{0.3} indicates the improved quality of the single crystals used in the current study.

Figure 2(b) compares EDCs recorded in the SC state at the k_F of the α' , β , and γ bands. We observe gap sizes of 1.7, 2.5, and 4.2 meV for the α' , β , and γ bands, respectively. We checked that the gap results obtained from the symmetrization coincide with the values estimated from the raw EDCs. Although multigap superconductivity has already been reported in other Fe-based systems,^{1–4,13,14} it is the first time that a SC gap larger at the M point than at the Γ point is observed in a Fe-based superconductor, with the exception of the 122-chalcogenides, which do not have Γ -centered holelike FSs at all.^{7–9,15}

Whether gap nodes exist at the M point or not in the SC state is a highly debated issue in the study of Fe-based superconductors. A previous angle-resolved specific heat (ARSH) experiment claims nodes or minimal gaps in FeTe_{0.55}Se_{0.45} samples.¹⁶ To check this point we performed

high-energy resolution k -dependence measurements on both Γ - and M-centered FS pockets. Figures 2(c) and 2(d) show the symmetrized EDCs of the β and γ bands, respectively, at different k_F positions indicated on the FS displayed in Fig. 2(e). As illustrated by the polar plot in Fig. 2(f), the gap sizes on both pockets are nodeless and quite isotropic, with error bars limiting possible anisotropy to 15%.

It has been proposed that the orbital character may be important to determine the pairing strength and the symmetry for this multiorbital system.^{17,18} Figures 3(a) and 3(b) show intensity plots along Γ -M under S polarization and P polarization, respectively. We observed that the α' band is enhanced under S polarization, but is significantly suppressed by P polarization. The α band, however, has reversed response under S and P polarizations. The same behavior has been observed in a previous ARPES study for the α and α' bands along Γ -X.¹⁹ This suggests that the α (α') band has an even (odd) symmetry along both Γ -M and Γ -X. Similarly, we determine that the β band is even along Γ -X but odd along Γ -M, in agreement with previous reports.^{19,20} Taking LDA calculations as reference,^{19–21} we reach the following conclusion on the orbital characters for the three bands observed around Γ , which is summarized in Fig. 3(c): the β band has mainly a d_{xy} orbital character, whereas the α (α') band is mainly the even (odd) combination of the d_{xz} and d_{yz} orbitals [labeled as d_{even} (d_{odd})]. Therefore, we conclude that the 2.5 and 1.7 meV gaps at

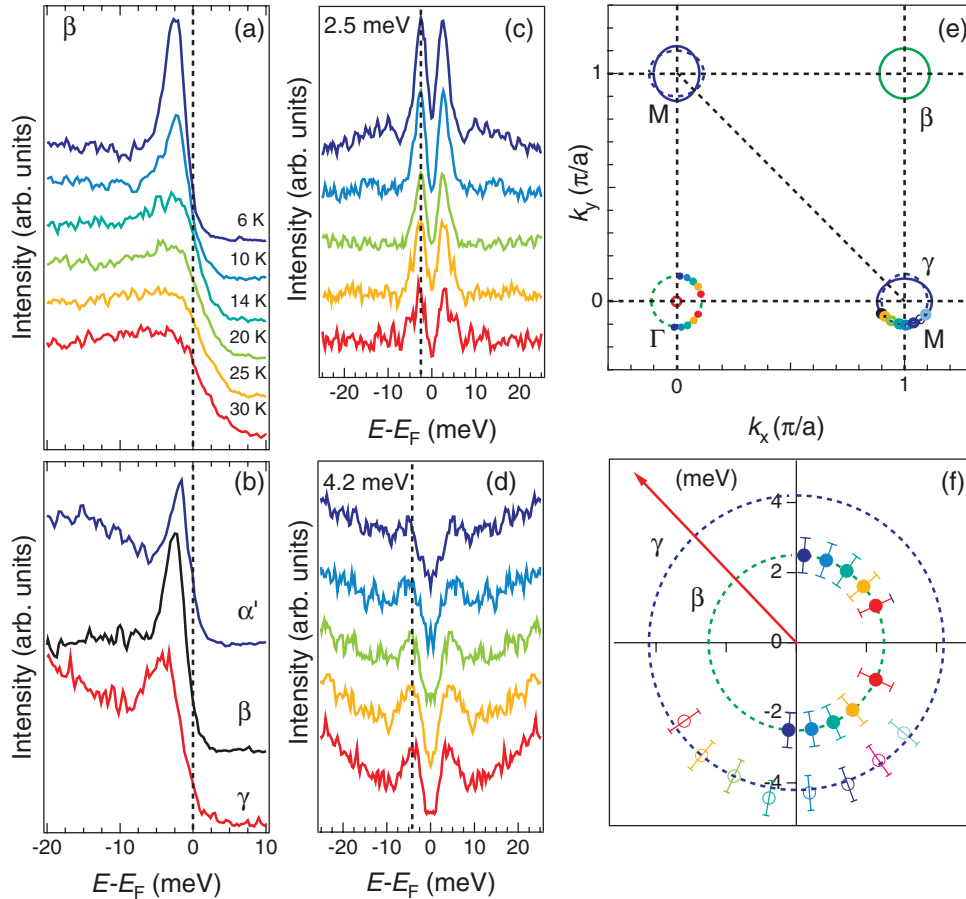


FIG. 2. (Color online) (a) Temperature dependence of the SC gap of the β band. (b) Comparison of the SC gaps of the α' , β , and γ bands. (c) and (d) k dependence of symmetrized EDCs along the β and γ FSs, respectively. (e) Schematic FS indicating positions where the SC gap size has been measured. Dotted FSs are folded from the BZ of a pure Fe plane due to the alternate position of the chalcogen atoms above and below the Fe plane. (f) Polar plot of the SC gaps with dotted circles indicating the average values on each FS pocket.

Γ originate from the d_{xy} and d_{xz}/d_{yz} orbitals, respectively. As mentioned above, the α band top is 14 meV away from E_F and is thus slightly separated from the α' band top. This contradicts the LDA expectation of degeneracy of the d_{even} and d_{odd} bands at Γ preserved by the fourfold symmetry. Careful examination from LDA calculations reveals a possible Se/Te p_z band situation around the BZ center, complicating the band dispersion around Γ . We note that the small gap of 1.7 meV at the Γ point may be related to at least partly to the Se/Te p_z orbital, rather than purely to the Fe $3d$ orbitals that generate stronger pairing.

Figure 3(d) shows comparison of our ARPES EDC spectra and a STM conductance curve measured on similar $\text{FeTe}_{1-x}\text{Se}_x$ ($T_c \sim 14.5$ K).²² The three gaps observed by ARPES can find corresponding features in the STM data. The smallest gap of 1.7 meV observed at Γ matches well the 1.8 meV peak in the STM curve. The 4.2 meV gap observed on the electron FS and the 2.5 meV gap on the β hole FS correspond well to the 4 meV peak and the weak 2.5 meV shoulder in the STM curve, respectively. We further compare our results with optical measurements²³ on the same sample batch, as shown in Fig. 3(e). We find a good consistency of gap size that excludes surface contribution in our observations. It is important to point out that samples cleave between

two equivalent weakly bonded Se(Te) planes, exposing a nonpolar surface which is usually bulk representative. The bulk nature is also reflecting from the ARPES observation that the SC gap and coherence diminish right at the bulk T_c , as demonstrated by Fig. 2(a). In addition, inelastic neutron scattering (INS) measurements have revealed a resonant mode around 6–7 meV in the SC state of samples with similar T_c and composition.²⁴ We note that the sum of the gaps on the β and γ FSs (6.7 meV) is compatible to the energy of the resonant mode, suggesting that it may be related to scattering between the β hole FS and the γ electron FS.

Assuming that high magnetic field does not change the topology of the FS and the SC gap function, the contrast between highly anisotropic gaps suggested by ARSH experiments¹⁶ and isotropic gaps observed by ARPES is puzzling. Even though nodes at a particular k_z is still possible, the quasi-two dimensionality of this $\text{FeTe}_{1-x}\text{Se}_x$ material makes this scenario unlikely. Another possible cause is that the cleaved surface may have enhanced impurity scattering tending to average out possible gap anisotropy, which is also unlikely since isotropic gaps have been observed by ARPES for different structures of Fe-based superconductors with different surfaces exposed. We note that the very sharp SC coherent peaks in this material indicate weak scattering effect,

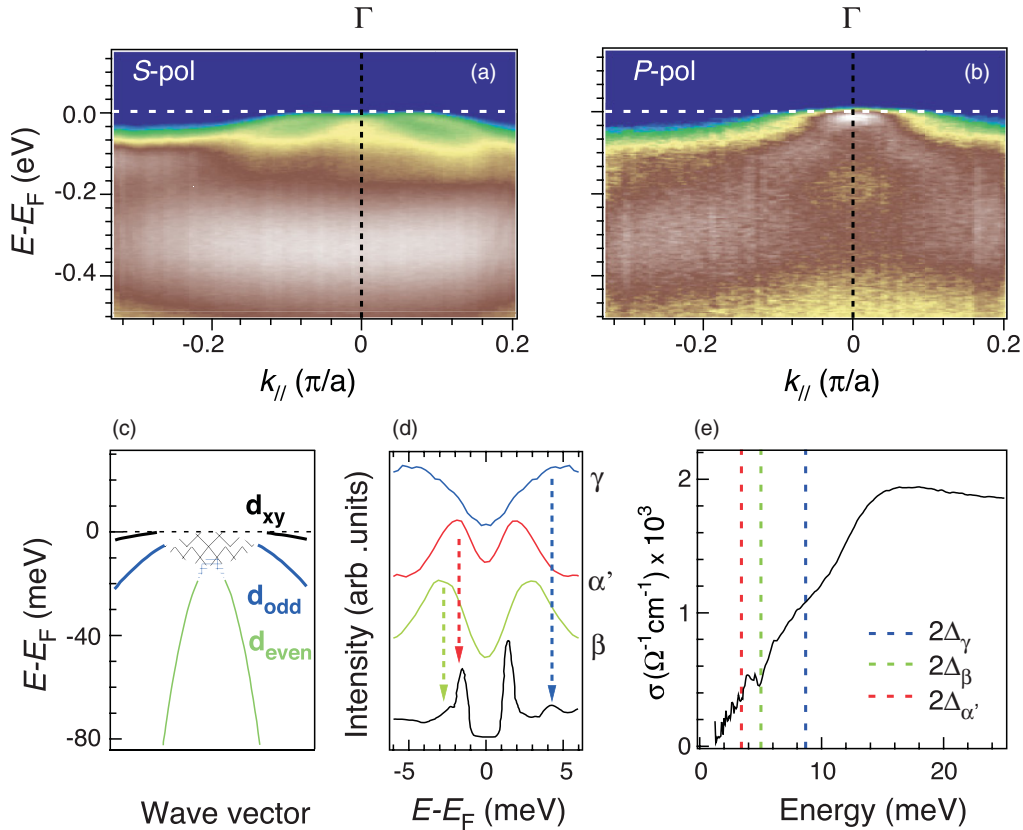


FIG. 3. (Color online) (a) and (b) ARPES intensity plots along the Γ -M high-symmetry line measured with S and P polarizations, respectively. (c) Schematic band structure and dominant orbital character of each band at Γ . (d) SC gap correspondence between ARPES and STM measurements. Blue, red, and green lines are k_F symmetrized EDCs of the α' , β , and γ band, respectively. Dashed arrows indicate the correspondence between ARPES and STM (black curve, from Ref. 22) features. (e) Comparison of ARPES data with optical conductivity (black curve, from Ref. 23). Colored dashed lines position the 2Δ values of α' , β , and γ band, respectively.

and that small linewidth broadening induced by impurities does not usually shift the quasiparticle peak position, or the gap value observed by ARPES. However, it may affect some thermodynamics measurements that are sensitive to the residual density of states. In addition, we point out that transport measurements may be more sensitive to the overall gap distribution, which is anisotropic with respect to the Γ point because of the FS topology itself, rather than to the detail of the gap distribution around each FS taken separately.

Interestingly, the gap amplitude is stronger on the electron FS, as shown in Fig. 4(a). In contrast, ferropnictide superconductors have similar gap size on the quasi-nested holelike and electronlike FSs,^{1-3,14} which can be captured by the simple s_{\pm} gap function $\cos k_x \cos k_y$ naturally derived from the effective J_1 - J_2 model,²⁵ where J_1 and J_2 are the nearest- and next-nearest-neighbor magnetic exchange interaction strengths, respectively. Figure 4(b) shows that a simple $\cos k_x \cos k_y$ function cannot fit the gaps on both hole and electron FSs. However, the exchange parameters in ferrochalcogenides differ from the ones in ferropnictides in such a way that (i) $J_1 < 0$ (ferromagnetic) and (ii) J_3 (next-next-nearest-neighbor exchange) is no longer negligible. A sizable AF J_3 (~ 7 meV) that may play a critical role in forming the bicollinear magnetic pattern in FeTe was

reported from INS measurements.¹⁰ The s -wave pairing form induced by AF J_3 is $\Delta_3(\cos 2k_x + \cos 2k_y)/2$. Combined with $\cos k_x \cos k_y$ induced by AF J_2 , the pairing form in this material should be $|\Delta_2 \cos k_x \cos k_y - \Delta_3(\cos 2k_x + \cos 2k_y)/2|$. As demonstrated in Fig. 4(c), this gap function fits all gaps reasonably well, with $\Delta_2 = 3.55$ meV and $\Delta_3 = 0.95$ meV. The ratio between Δ_2 and Δ_3 is similar with J_2/J_3 (22/7) given by an INS study.¹⁰ We note that the small gap of 1.7 meV at Γ would fall slightly off the fitting curve, as expected if the α' band hybridizes with Se $4p_z$ states.

Stronger and isotropic pairing on the electron FS sheets of $\text{FeTe}_{1-x}\text{Se}_x$ has important implications to superconductivity in another ferrochalcogenide, AFe_2Se_2 ($A = \text{K, Rb, Cs, Tl}$), with T_c as high as 31 K.^{26,27} Several ARPES studies⁷⁻⁹ revealed an isotropic SC gap on its electron FS. Interestingly, the $2\Delta/T_c$ ratios are similar in these two ferrochalcogenides (7 in AFe_2Se_2 ⁷ vs 6.7 in $\text{FeTe}_{1-x}\text{Se}_x$). A recent INS study indicates a large $J_3 \sim 9$ meV for $\text{K}_{0.8}\text{Fe}_{1.6}\text{Se}_2$ as well.²⁸ We propose that AFe_2Se_2 and $\text{FeTe}_{1-x}\text{Se}_x$ belong to a same class as far as superconductivity is concerned, with the same pairing function: $|\Delta_2 \cos k_x \cos k_y - \Delta_3(\cos 2k_x + \cos 2k_y)/2|$. As shown in Fig. 4(d), the enhanced pairing on the electron FS around M accompanies the reduced pairing on the hole FS around Γ . For AFe_2Se_2 , which does not have hole FS at Γ , this effect may

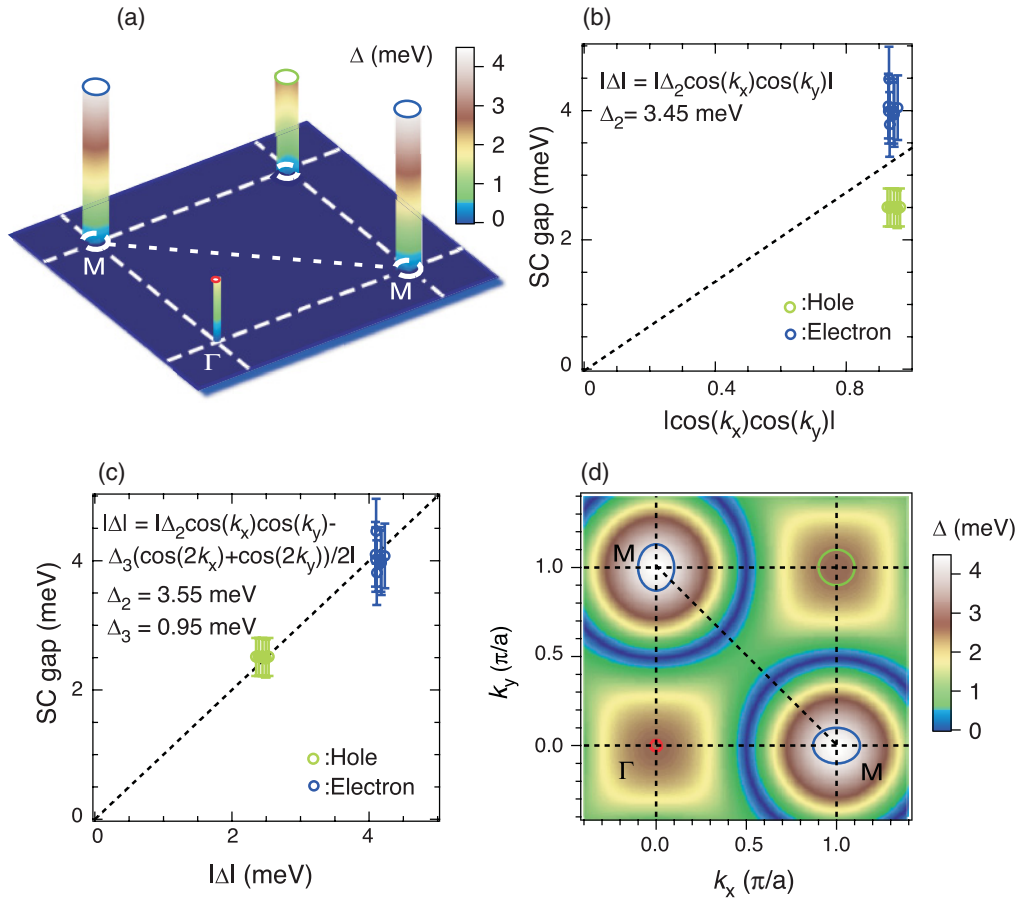


FIG. 4. (Color online) (a) 3D representation of the SC gap with the FS topology. (b) Fit of the SC gap data with a $|\Delta_2 \cos k_x \cos k_y|$ gap function. (c) Fit of the SC gap data with a $|\Delta_2 \cos k_x \cos k_y - \Delta_3(\cos 2k_x + \cos 2k_y)/2|$ gap function. The horizontal and vertical error bars represent the uncertainties on k_F positions and their corresponding SC gap values. (d) In-plane k distribution of the $|\Delta_2 \cos k_x \cos k_y - \Delta_3(\cos 2k_x + \cos 2k_y)/2|$ SC gap function along with the FSs.

have no impact on T_c . Clearly, the observation of isotropic SC gaps with strong pairing on the electronlike FS pocket in the ferroselenides supports the strong coupling local pairing picture for Fe-based superconductors.

IV. CONCLUSION

In conclusion, we reported high resolution ARPES results on $\text{FeTe}_{0.55}\text{Se}_{0.45}$ SC single crystal samples. The SC gaps on both holelike and electronlike FSs are isotropic. More importantly, a larger SC gap on the electronlike FS is observed. The stronger pairing strength on electronlike FS is naturally explained by the enhanced AF magnetic exchange between third nearest neighbors (J_3) in the chalcogenides as compared to the pnictides. Finally, the different SC gaps can be fitted by a single gap function that is fully consistent with the strong coupling J_1 - J_2 - J_3 approach.

ACKNOWLEDGMENTS

We acknowledge B. A. Bernevig, A. Chubukov, Z. Fang, D.-H. Lee, H.-H. Wen, and G. Xu for valuable discussions, T. Kawahara for his help in the experiments, and T. Hanaguri and C. Homes for providing STM and optical conductivity data, respectively. This work was supported by grants from Chinese Academy of Sciences (2010Y1JB6), Ministry of Science and Technology of China (2010CB923000 and 2011CBA00101), Chinese National Science Foundation (11004232 and 11050110422), JSPS, TRiP-JST, MEXT of Japan, CREST-JST and National Science Foundation (Contract No. DE-AC02-05CH11231). The Synchrotron Radiation Center, University of Wisconsin-Madison, and at the National Light Source of Brookhaven National Laboratory, are supported by the National Science Foundation under Award No. DMR-0537588, and by the Department of Energy of USA under Contract No. DE-AC02-98CH10886, respectively.

*dingh@iphy.ac.cn

¹H. Ding, P. Richard, K. Nakayama, K. Sugawara, T. Arakane, Y. Sekiba, A. Takayama, A. Souma, T. Sato, T. Takahashi, Z. Wang, X. Dai, Z. Fang, J. L. Luo, and N. L. Wang, *Europhys. Lett.* **83**, 47001 (2008).

²K. Nakayama, T. Sato, P. Richard, Y.-M. Xu, Y. Sekiba, S. Souma, G. F. Chen, J. L. Luo, N. L. Wang, H. Ding, and T. Takahashi, *Europhys. Lett.* **85**, 67002 (2009).

³L. Zhao, H. Y. Liu, W. T. Zhang, J. Q. Meng, X. W. Jia, G. D. Liu, X. L. Dong, G. F. Chen, J. L. Luo, N. L. Wang, G. L. Wang, Y.

- Zhou, Y. Zhu, X. Y. Wang, Z. X. Zhao, Z. Y. Xu, C. T. Chen, and X. J. Zhou, *Chin. Phys. Lett.* **25**, 4402 (2008).
- ⁴K. Terashima, Y. Sekiba, J. H. Bowen, K. Nakayama, T. Kawahara, T. Sato, P. Richard, Y.-M. Xu, L. J. Li, G. H. Cao, Z.-A. Xu, H. Ding, and T. Takahashi, *Proc. Natl. Acad. Sci. USA* **106**, 7330 (2009).
- ⁵T. Qian, N. Xu, Y.-B. Shi, K. Nakayama, P. Richard, T. Kawahara, T. Sato, T. Takahashi, M. Neupane, Y.-M. Xu, X.-P. Wang, G. Xu, X. Dai, Z. Fang, P. Cheng, H.-H. Wen, and H. Ding, *Phys. Rev. B* **83**, 140513(R) (2011).
- ⁶W. Bao, Y. Qiu, Q. Huang, M. A. Green, P. Zajdel, M. R. Fitzsimmons, M. Zhernenkov, S. Chang, M. H. Fang, B. Qian, E. K. Vehstedt, J. Yang, H. M. Pham, L. Spinu, and Z. Q. Mao, *Phys. Rev. Lett.* **102**, 247001 (2009).
- ⁷X.-P. Wang, T. Qian, P. Richard, P. Zhang, J. Dong, H.-D. Wang, C.-H. Dong, M.-H. Fang, and H. Ding, *Europhys. Lett.* **93**, 57001 (2011).
- ⁸Y. Zhang, L. X. Yang, M. Xu, Z. R. Ye, F. Chen, C. He, H. C. Xu, J. Jiang, B. P. Xie, J. J. Ying, X. F. Wang, X. H. Chen, J. P. Hu, M. Matsunami, S. Kimura, and D. L. Feng, *Nat. Mater.* **10**, 273 (2011).
- ⁹D. Mou, S. Liu, X. Jia, J. He, Y. Peng, L. Zhao, L. Yu, G. Liu, S. He, X. Dong, J. Zhang, H. Wang, C. Dong, M. Fang, X. Wang, Q. Peng, Z. Wang, S. Zhang, F. Yang, Z. Xu, C. Chen, and X. J. Zhou, *Phys. Rev. Lett.* **106**, 107001 (2011).
- ¹⁰O. J. Lipscombe, G. F. Chen, Chen Fang, T. G. Perring, D. L. Abernathy, A. D. Christianson, Takeshi Egami, N. L. Wang, J. P. Hu, and P. C. Dai, *Phys. Rev. Lett.* **106**, 057004 (2011).
- ¹¹C. Fang, Y.-L. Wu, R. Thomale, B. A. Bernevig, and J. P. Hu, *Phys. Rev. X* **1**, 011009 (2011).
- ¹²K. Nakayama, T. Sato, P. Richard, T. Kawahara, Y. Sekiba, T. Qian, G. F. Chen, J. L. Luo, N. L. Wang, H. Ding, and T. Takahashi, *Phys. Rev. Lett.* **105**, 197001 (2010).
- ¹³S. V. Borisenko, V. B. Zabolotnyy, D. V. Evtushinsky, T. K. Kim, I. V. Morozov, A. N. Yaresko, A. A. Kordyuk, G. Behr, A. Vasiliev, R. Follath, and B. Buchner, *Phys. Rev. Lett.* **105**, 067002 (2010).
- ¹⁴Z.-H. Liu, P. Richard, K. Nakayama, G.-F. Chen, S. Dong, J.-B. He, D.-M. Wang, T.-L. Xia, K. Umezawa, T. Kawahara, S. Souma, T. Sato, T. Takahashi, T. Qian, Y. Huang, N. Xu, Y. Shi, H. Ding, and S.-C. Wang, *Phys. Rev. B* **84**, 064519 (2011).
- ¹⁵T. Qian, X.-P. Wang, W.-C. Jin, P. Zhang, P. Richard, G. Xu, X. Dai, Z. Fang, J.-G. Guo, X.-L. Chen, and H. Ding, *Phys. Rev. Lett.* **106**, 187001 (2011).
- ¹⁶B. Zeng, G. Mu, H. Q. Luo, T. Xiang, I. I. Mazin, H. Yang, L. Shan, C. Ren, P. C. Dai, and H.-H. Wen, *Nat. Commun.* **1**, 112 (2010).
- ¹⁷S. Graser, T. A. Maier, P. J. Hirschfeld, and D. J. Scalapino, *New J. Phys.* **11**, 025016 (2009).
- ¹⁸I. I. Mazin and J. Schmalian, *Physica C* **469**, 614 (2009).
- ¹⁹F. Chen, B. Zhou, Y. Zhang, J. Wei, H.-W. Ou, J.-F. Zhao, C. He, Q.-Q. Ge, M. Arita, K. Shimada, H. Namatame, M. Taniguchi, Z.-Y. Lu, J. P. Hu, X.-Y. Cui, and D. L. Feng, *Phys. Rev. B* **81**, 014526 (2010).
- ²⁰A. Tamai, A. Y. Ganin, E. Rozbicki, J. Bacsá, W. Meevasana, P. D. C. King, M. Caffio, R. Schaub, S. Margadonna, K. Prassides, M. J. Rosseinsky, and F. Baumberger, *Phys. Rev. Lett.* **104**, 097002 (2010).
- ²¹A. Subedi, L. Zhang, D. J. Singh, and M. H. Du, *Phys. Rev. B* **78**, 134514 (2008).
- ²²T. Hanaguri, S. Niitaka, K. Kuroki, and H. Takagi, *Science* **328**, 474 (2010).
- ²³C. C. Homes, A. Akrap, J. S. Wen, Z. J. Xu, Z. W. Lin, Q. Li, and G. D. Gu, *Phys. Rev. B* **81**, 180508(R) (2010).
- ²⁴Y. Qiu, W. Bao, Y. Zhao, C. Broholm, V. Stanev, Z. Tesanovic, Y. C. Gasparovic, S. Chang, J. Hu, B. Qian, M.-H. Fang, and Z. Q. Mao, *Phys. Rev. Lett.* **103**, 067008 (2009).
- ²⁵K. Seo, B. A. Bernevig, and J. P. Hu, *Phys. Rev. Lett.* **101**, 206404 (2008).
- ²⁶J. Guo, S. Jin, G. Wang, S. Wang, K. Zhu, T. Zhou, M. He, and X.-L. Chen, *Phys. Rev. B* **82**, 180520(R) (2010).
- ²⁷M.-H. Fang, H. D. Wang, C. H. Dong, Z. J. Li, C. M. Feng, J. Chen, and H. Q. Yuan, *Europhys. Lett.* **94**, 27009 (2011).
- ²⁸M. Wang, C. Fang, D.-X. Yao, G. T. Tan, L. W. Harriger, Y. Song, T. Netherton, C. L. Zhang, M. Wang, M. B. Stone, W. Tian, J. P. Hu, and P. C. Dai, *Nat. Commun.* **2**, 580 (2011).